Chapter 2

Scale transition methods

2.1 Scale separation

Consider a structure made of a composite material. At the level of this structure (macroscopic level), the material is seen as homogeneous. Imposed loads on the structure with prescribed displacements on a part Γ_U of the boundary and prescribed tractions on the remaining part Γ_F induce strain and stress fields in the material. At each macroscopic point, the relation linking local strain and stress depends on the heterogeneous microstructure, which can be seen at a smaller scale only. In order to take into account this heterogeneous microstructure, a representative volume element (RVE) of it is defined at each macroscopic point (see figure 2.1)[1]. When linking these scales, several problems arise. Among them: how to load the RVE from the applied macroscopic strain or stress at the corresponding macroscopic point, solve the boundary value problem on the RVE and compute the corresponding macroscopic response. First of all, precisions on the scale separation must be given. For this, following Zaoui [110], let's define various length scales in an ascending order:

- d_0: lower length bound under which continuum mechanics is no more valid.
- d: characteristic size of the heterogeneities.
- l: size of the RVE.
- λ: fluctuation length of the prescribed mechanical loading over the structure.

[1] A simple definition of the RVE was given by Drugan and Willis [28]: "*It is the smallest material volume element of the composite for which the usual spatially constant (overall modulus) macroscopic constitutive representation is a sufficiently accurate model to represent mean constitutive response*".

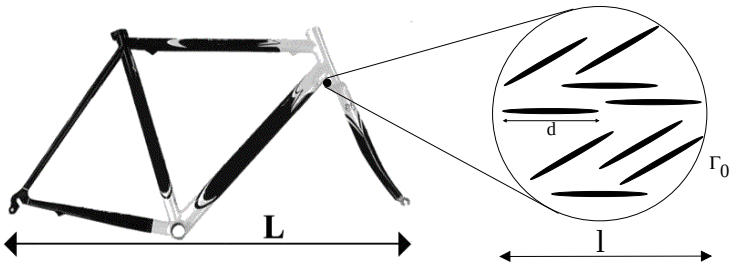

Figure 2.1: Scale separation and characteristic length scales: the material is viewed as homogeneous at the macroscopic level while heterogeneities can be seen at the level of the RVE.

- L: characteristic size of the structure.

In order to consider the structure as a continuum medium, the size of the RVE must be much smaller than the one of the structure (i.e.: $l \ll L$). Furthermore, as a macroscopic point is viewed as the center of the RVE and the response of the boundary value problem is macroscopically homogeneous, characteristic size of the heterogeneities must be much smaller than the size of the RVE (i.e.: $d \ll l$). Moreover, continuum mechanics remains valid at the scale of the RVE so that $d_0 \ll d$. Finally, the size of the RVE must be much smaller than the fluctuation length of the prescribed mechanical loading of the whole body (i.e.: $l \ll \lambda$) so that the use of the classical integral and differential tools of structural analysis remains valid.

Defining the RVE is not an easy task since the microstructure is not necessary known a priori. In the case of random microstructure (figure 2.2a), the property $d \ll l$ is taken into account so that a fictitious random microstructure of the RVE might be generated in order to give a significant response from a statistical point of view. Evidently, when generating a geometry, all the available information of the microstructure must be taken into account (volume fraction of each phase, orientations and shape of the inclusions,...). Periodic microstructures (figure 2.2b) are particularly suitable for numerical simulations on a unit cell. With the help of the geometrical periodicity, one can define a unit cell on which a well-posed problem is solved. In the case of random microstructure, defining the minimum size of the RVE is a crucial problem. Many papers discuss this subject and the minimum required size depends on several factors including the observed property, the geometry, the volume fraction and the mechanical (and thermal) behavior (see Povirk [88] and Kanit *et al.* [50] who define mathematical criteria to fix the cell size). Sometimes, microstructural arrangements (figure 2.2c) enable to strongly reduce the size of the unit cell. If assumptions are required to define such unit cell, different arrangements can sometimes be considered which lead to different predictions of the behavior.

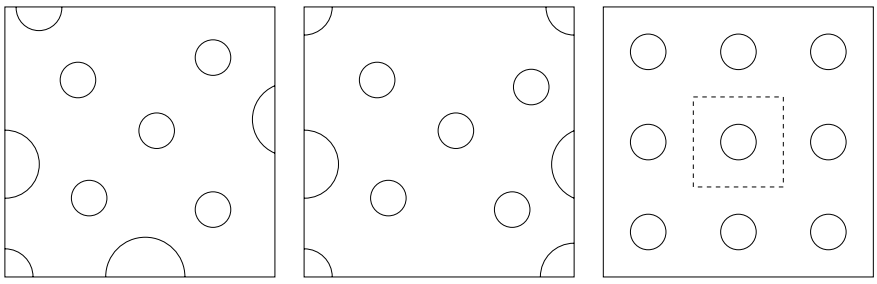

(a) RVE with a random microstructure.

(b) Periodic unit cell with random microstructure.

(c) Periodic unit cell and microstructural arrangements.

Figure 2.2: Periodicity of the unit cell and the microstructural arrangements.

Also, either on the RVE or the periodic unit cell, various boundary conditions might apply which will also influence the predictions.

2.2 Linking macroscopic and microscopic scales

This section explains how to perform the scale transition between macroscopic and microscopic levels. More precisely, from the load (strain or stress) defined at each point of the macroscopic level (e.g. at integration points of a finite element mesh of the structure), which boundary conditions must be applied to the corresponding RVE. For this, averaging theorems are required and recalled hereafter.

2.2.1 On averages

A macroscopic property can be defined as the volume average of that property over the whole RVE. Mathematically, this reads:

$$\bar{\boldsymbol{f}} =< \boldsymbol{f}(x) >_{\omega} = \frac{1}{V}\int_{\omega} \boldsymbol{f}(\boldsymbol{x})dV, \tag{2.1}$$

where $\boldsymbol{x}$ is the position vector in a local frame attached to the RVE ω of volume V.

Strain averages

Let's define the macroscopic strain as the volume average of the microscopic strain:

$$\bar{\boldsymbol{\varepsilon}} =< \boldsymbol{\varepsilon}(\boldsymbol{x}) >_{\omega} = \frac{1}{V}\int_{\omega} \boldsymbol{\varepsilon}(\boldsymbol{x})\mathrm{d}V. \tag{2.2}$$

By definition of a strain tensor and using the divergence theorem, the last expression can be rewritten in a Cartesian frame as (dependence of the local fields with respect to $\boldsymbol{x}$ is omitted for clarity):

$$\bar{\varepsilon}_{ij} = \frac{1}{2V}\int_{\omega}\left(\frac{\partial u_i}{\partial x_j}+\frac{\partial u_j}{\partial x_i}\right)\mathrm{d}V = \frac{1}{2V}\int_{\partial\omega}(u_i n_j + u_j n_i)\mathrm{d}A. \tag{2.3}$$

Stress averages

Let's define the macroscopic stress as the volume average of the microscopic stress:

$$\bar{\boldsymbol{\sigma}} = <\boldsymbol{\sigma}(\boldsymbol{x})>_{\omega} = \frac{1}{V}\int_{\omega}\boldsymbol{\sigma}(\boldsymbol{x})\mathrm{d}V. \tag{2.4}$$

Equilibrium equations without body forces (i.e. the stress field is equilibrated, $\nabla.\boldsymbol{\sigma} = \mathbf{0}$) combined to the divergence theorem enable to rewrite the last expression in a Cartesian frame as (dependence of the local fields with respect to $\boldsymbol{x}$ is omitted for clarity):

$$\bar{\sigma}_{ij} = \frac{1}{V}\int_{\omega}\frac{\partial(\sigma_{ik}x_j)}{\partial x_k}\mathrm{d}V = \frac{1}{V}\int_{\partial\omega}t_i x_j \mathrm{d}A. \tag{2.5}$$

2.2.2 Imposition of the boundary conditions

In this section, a coherent scale transition with the averaging theorems is proposed for several boundary conditions imposed on the RVE. Three of them are presented: prescribed displacements, prescribed tractions and periodic boundary conditions which are valid for periodic unit cells (figure 2.2b).

Linear displacements. In the case of prescribed displacement boundary conditions, displacement of each point on the boundary $\partial\omega$ of the RVE is given by:

$$\boldsymbol{u}_i(\boldsymbol{x}) = G_{ij}\boldsymbol{x}_j \text{ with } \boldsymbol{x} \text{ on } \partial\omega, \tag{2.6}$$

where $\boldsymbol{G}$ is the displacement gradient tensor so that the strain tensor $\boldsymbol{\varepsilon}$ is its symmetric part: $\boldsymbol{\varepsilon} = \frac{1}{2}\left(\boldsymbol{G}+\boldsymbol{G}^T\right)$. If a uniform displacement gradient $\boldsymbol{G}^0$ corresponding to a strain tensor $\boldsymbol{\varepsilon}^0$ is used to impose the displacements, equation (2.3) reads:

$$\begin{aligned}
\bar{\varepsilon}_{ij} &= \frac{1}{2V}\left[\boldsymbol{G}^0_{ik}\int_{\partial\omega}x_k n_j \mathrm{d}A + \boldsymbol{G}^0_{jk}\int_{\partial\omega}x_k n_i \mathrm{d}A\right] &(2.7)\\
&= \frac{1}{2V}\left[\boldsymbol{G}^0_{ik}\int_{\omega}\frac{\partial x_k}{\partial x_j}\mathrm{d}V + \boldsymbol{G}^0_{jk}\int_{\omega}\frac{\partial x_k}{\partial x_i}\mathrm{d}V\right]\\
&= \varepsilon^0_{ij}. &(2.8)
\end{aligned}$$

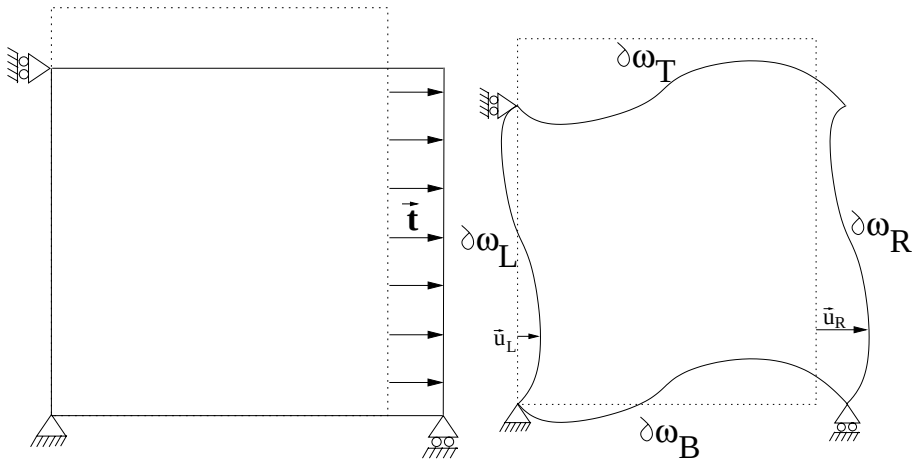

(a) Prescribed uniaxial tractions. (b) Periodic boundary conditions.

Figure 2.3: Imposition of boundary conditions to a 2D rectangular RVE. Initial configuration is in dots and final one in continuous lines.

Imposing linear displacements indeed satisfies the strain averaging relation (2.2) if $\bar{\boldsymbol{\varepsilon}}$ is used to compute the prescribed displacements.

Uniform tractions. For prescribed traction boundary conditions, imposed traction at each point on the boundary of the RVE is given by (see figure 2.3a):

$$\boldsymbol{t}(\boldsymbol{x}) = \boldsymbol{\sigma}^T.\boldsymbol{n}(\boldsymbol{x}) \text{ with } \boldsymbol{x} \text{ on } \partial\omega, \tag{2.9}$$

where superscript ^{T} stands for transposition and $\boldsymbol{n}$ for the outer normal at point $\boldsymbol{x}$. If a uniform stress tensor $\boldsymbol{\sigma}^0$ is used to impose the tractions, expression (2.5) reads:

$$\bar{\sigma}_{ij} = \frac{1}{V}\sigma^0_{ik}\int_{\partial\omega} n_k x_j \mathrm{d}A = \frac{1}{V}\sigma^0_{ik}\int_{\omega}\frac{\partial x_j}{\partial x_k}\mathrm{d}V = \sigma^0_{ij}. \tag{2.10}$$

Imposing uniform tractions indeed satisfies the stress averaging relation (2.4) if $\bar{\boldsymbol{\sigma}}$ is used to compute the prescribed tractions. If the finite element method is used to solve the problem on the macroscopic structure, prescribed tractions on the boundary of the RVE cannot apply directly since finite element codes are generally strain driven. Furthermore, one has to be careful when using both finite strains and prescribed traction boundary conditions since rotations must be taken into account in order to determine uniquely the corresponding strain (Kouznetsova [51]).

Periodic boundary conditions. A third possibility is to consider periodic boundary conditions. In this case, due to the repetition of the cell in all di-

rections before and after application of the load, periodic deformations and anti-periodic tractions are applied at each corresponding pair of nodes lying on opposite faces of the RVE boundary (see figure 2.3b):

$$\boldsymbol{u}_R - \boldsymbol{u}_L = \boldsymbol{G}.(\boldsymbol{x}_R - \boldsymbol{x}_L), \tag{2.11}$$

$$\boldsymbol{t}_R = -\boldsymbol{t}_L. \tag{2.12}$$

Imposing periodic boundary condition also satisfies (2.2) if the displacement gradient $\boldsymbol{G}$ is computed from $\boldsymbol{\varepsilon} = \bar{\boldsymbol{\varepsilon}}$. The proof is similar to (2.7-2.8) excepted that the integrals must be split into two parts corresponding to the opposite faces.

Solving the RVE boundary value problem with given macroscopic strain or stress does not necessarily give the same response but generally surrounds the correct response. The larger the dimension of the cell is with respect to the size of its constituents, the closest these two responses are. Periodic boundary conditions generally lead to an intermediate and more accurate response, which means that a smaller cell size can be considered. This result is represented schematically on figure 2.4. This is even more true during an analysis of the microscopic fields. Prescribed displacements or tractions on the boundary give an inaccurate response close to the boundaries (e.g.: if uniform tractions are prescribed, the stress will be uniform on the faces which is obviously not correct). On the contrary, when imposing periodic boundary conditions, the treatment of the lateral faces is exactly the same as the one of a section in the middle of the RVE. These facts have been observed numerically in numerous studies, including Kanit *et al.* [50] in linear elasticity, Jiang *et al.* [46, 47] in elasto-plasticity and Ostoja-Starzewski [73] for a wide range of constitutive behaviors.

2.2.3 Hill's Lemma

Given an equilibrated stress field $\boldsymbol{\sigma}$, compatible deformations $\boldsymbol{\varepsilon}$ (i.e.: $\boldsymbol{\varepsilon} = \boldsymbol{\varepsilon}(\boldsymbol{u})$) and either the stress field, either the strain field satisfies one of the three boundary conditions defined in section 2.2.2, Hill's lemma reads:

$$< \boldsymbol{\sigma} : \boldsymbol{\varepsilon} >_\omega = < \boldsymbol{\sigma} >_\omega : < \boldsymbol{\varepsilon} >_\omega . \tag{2.13}$$

Up to now, no hypothesis has been made on an eventual link between stresses and strains. If they are coupled through a constitutive law, the lemma insures the equality between the average of the microscopic work $\boldsymbol{\sigma} : \boldsymbol{\varepsilon}$ and the macroscopic work $\bar{\boldsymbol{\sigma}} : \bar{\boldsymbol{\varepsilon}}$. This result is commonly called *Hill-Mandel condition* or *macrohomogeneity condition*.

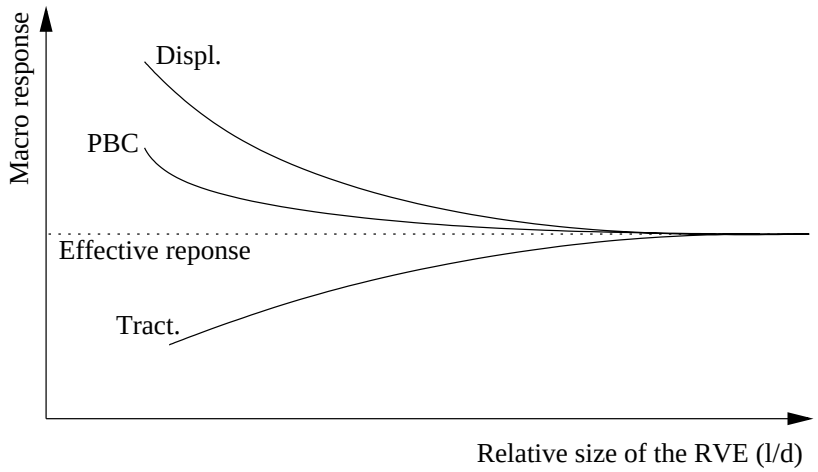

Figure 2.4: Accuracy of the predictions with respect to the RVE size for different boundary conditions (Displ.: prescribed displacements, PBC: periodic boundary conditions, Tract.: prescribed tractions).

2.2.4 Prediction of the macroscopic response

Solving the boundary value problem over the RVE is the core of this work. Several solution methods are proposed in section 2.3. Once this problem is solved, the macroscopic response still must be computed. A coherent manner to predict it is through a volume-average over the RVE so that Hill-Mandel condition is satisfied. If prescribed displacements or periodic boundary conditions are applied, this reads:

$$\bar{\boldsymbol{\sigma}} = \frac{1}{V}\int_{\omega} \boldsymbol{\sigma}(x) dV. \tag{2.14}$$

If prescribed traction boundary conditions are applied, the macroscopic strain is computed as:

$$\bar{\boldsymbol{\varepsilon}} = \frac{1}{V}\int_{\omega} \boldsymbol{\varepsilon}(x) dV. \tag{2.15}$$

2.3 Various approaches to solve the scale transition problem

The micro/macro problem being defined, the boundary value problem over the RVE must still be solved. For this, several approaches have been proposed over the years, some of them being reported hereafter. Several criteria must be taken

into account when choosing a solution method: arrangement and periodicity of the microstructure, computational cost, desired information on the local fields, accuracy of the predictions,... A comparison of all the presented methods is given at the end of this section.

2.3.1 Finite element methods

Solving the boundary value problem on a RVE can be done by a classical finite element approach. If periodic microstructure is assumed, unit cells are considered and periodic boundary conditions can apply. This method gives good results for both the global response and the local fields but has several disadvantages. One of them is, as most methods, the impossibility of taking into account of size effects. Also, generating good meshes for complex microstructures is difficult and its computational cost, especially if this problem is coupled to another one on the macroscopic structure, can be very high. Simplifications are sometimes required. One of them is to reduce the real three dimensional (3D) RVE to a simplified two dimensional (2D) axisymmetric or planar one. Since this method is the most accurate one, it has been adopted as validation tool in this work so that an entire chapter is dedicated to it (chapter 3). An alternative if difficulties in modeling the microstructure arise is the Voronoi cell finite element method. This approach initiated by Ghosh [35] is based on a Dirichlet tessellation of the microstructure into a network of multi-sided Voronoi polygons (see figure 2.5). This method is frequently used to represent the microstructure of polycrystals and sometimes for the one of two-phase materials (Kanit *et al.* [50]). In both cases, either regular or irregular meshes can be used, the latter being far better. Formulations in linear and some nonlinear regimes have been developed for these elements and applied to various constitutive behaviors. Another approach is the extended finite element approach (XFEM) for which shape functions are enriched so that it enables to deal with discontinuities of the displacement field. Main advantage is the generation of a more structured mesh since it does not have to fit boundaries of the heterogeneities.

2.3.2 Asymptotic homogenization method

The asymptotic homogenization method is an elegant technique for predicting both microscopic and macroscopic properties of heterogeneous media and was developed by Bensoussan *et al.* [6] and Sanchez-Palencia [89]. This method relies on a distinction between a characteristic length of the RVE (l) and the one of the real structure (L) so that the ratio of these lengths gives a very small number $\varepsilon = l/L$. Starting from the fact that a high level of heterogeneity in a periodic microstructure causes rapid variation of strains and stresses in a small neighborhood ε of a macroscopic point $\bar{\boldsymbol{x}}$, all variables are assumed to exhibit

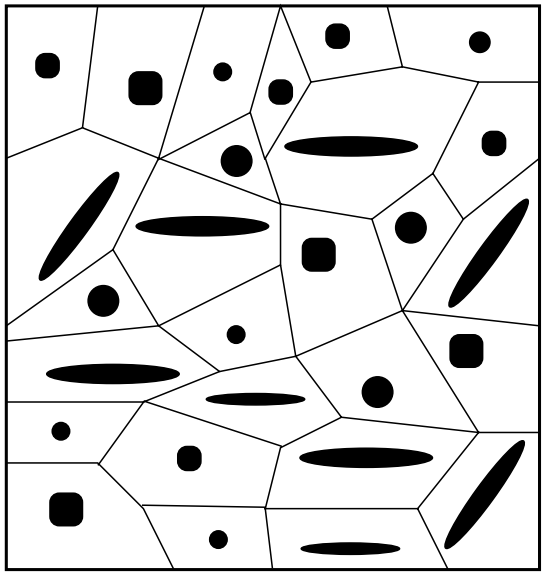

Figure 2.5: Tessellation of the microstructure into Voronoi cells.

dependence on both length scales of coordinates $\bar{\boldsymbol{x}}$ at the macroscopic level and $\bar{\boldsymbol{x}}/\varepsilon$ at the microscopic one (Ghosh *et al.* [36]). Asymptotical expansions of displacement and stress fields with respect to ε are introduced into equilibrium and constitutive relations. This leads to a set of partial differential equations with periodic boundary conditions which must be solved numerically (e.g. by Finite Element algorithms). This method has been applied successfully on linear elastic materials and is still under investigation for inelastic materials and damage. For a historical review of the method, see Chung *et al.* [21] and references therein. Notice that a combination of Voronoi cell tessellation and asymptotic homogenization methods has also been developed (Ghosh *et al.* [36]).

2.3.3 Generalized method of cells

The generalized method of cells enables to compute both microscopic and macroscopic properties of heterogeneous inelastic materials undergoing multi-axial mechanical loading as well as a spatially constant thermal loading. Following the review of Bednarcyk *et al.* [5], this method introduced by Aboudi [2], Paley and Aboudi [74] and Dvorak [29] (called the transformation field analysis) divides a repeating unit cell into an arbitrary number of generic cells,

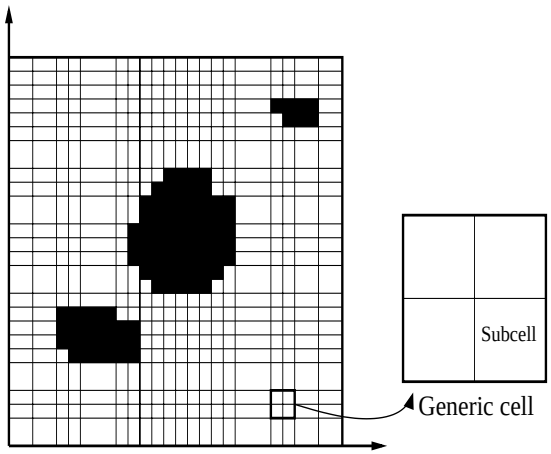

Figure 2.6: Typical discretization of a repeating unit cell, generic cell and subcell of the generalized method of cells.

themselves being divided into 4 (or 8) rectangular (or parallelepipedal) subcells and each one may contain a distinct homogeneous material (see figure 2.6). Basic assumption is that the displacement vector in each subcell varies linearly with the local subcell coordinates. Continuity of displacements and tractions between adjacent subcells and repeating unit cells is imposed. Global response is computed by a classical volume average. This method is very efficient in an algorithmic point of view and present a very good accuracy for the global response. However, due to the linear assumption of the displacement fields, quality of the local fields is not that high. In order to better capture the non-linearities, the high-fidelity general method of cells (Aboudi *et al.* [3, 4]) has been developed. Higher order displacement fields are used so that additional equations are needed to solve the system: the zeroth, first and second moments of the local (subcell) equilibrium equations must be satisfied in a volumetric sense. This induces a much higher computational cost than the original cell method but still lower than an equivalent finite element simulation. However, due to the imposed rectangular shape of the subcells, finite element methods generally still give a better accuracy of the microfields.

2.3.4 Fast Fourrier transform method

This meshless method introduced by Moulinec and Suquet [70, 71] makes use of the fast Fourrier transform to solve the problem at the microscopic level. Periodic boundary conditions are applied to the RVE so that the method is

limited to periodic microstructure. The RVE is digitalized into a given number of pixels (2D) or voxels (3D), different mechanical properties can be given to each of them. The method is thus particularly suitable for analyses of digital images of the real and eventually complex microstructure (clustering, percolation, ...). Constitutive and equilibrium equations can be written as an integral equation in which the Green tensor is introduced. Fourrier transform of this expression is easily obtained so that an iterative process over the stress tensor (if macroscopic strain is prescribed) to solve a nonlinear periodic equation (the Lippmann-Schwinger equation) in the Fourrier space is used. The adopted discretization is appropriate for the use of fast Fourrier transform packages. Solution is obtained at each pixel (or voxel) of the microstructure at a lower computational cost than a corresponding finite element simulation. Extensions to nonlinear behaviors require additional hypotheses. One possibility if the use of the generalized method of cells. This induces an additional subdivision of the phases and increases significantly the computational cost.

2.3.5 Mean-field homogenization schemes

Semi-analytical mean-field homogenization methods started several decades ago when computational cost was a real challenge. Based on assumptions of the interaction laws between the different phases (which define the homogenization scheme), they enable to give a macroscopic response as well as basic information on the state of deformation within the phases (i.e.: mean-field information). However, they are unable to predict any strain or stress localization on the contrary to other numerical approaches. Also, clustering, percolation and size effects cannot be taken into account. Most of these homogenization schemes are based on the Eshelby result [30], which is valid for ellipsoidal inclusions only and assume a perfect bonding between the constituents. Mean-field homogenization schemes were first developed for linear constituents and later extended to inelastic materials. They enable to get predictions of the macroscopic behavior as well as derivation of bounds. For nonlinear materials, a linearization of the local constitutive laws is required (formulation of the problem) in order to apply homogenization schemes valid in linear (thermo-)elasticity. The method is very efficient on a computational point of view and some models have a good accuracy in the linear elastic regime for both inclusion-reinforced materials and polycrystals. Extension of mean-field homogenization schemes to rate independent and dependent elasto-plastic behaviors is the main challenge of this work.

2.3.6 Comparison of the various methods

Here is a summary of the different capabilities and levels of accuracy offered by the homogenization methods presented above. Comparison is made over

several criteria, among them:

- Complex geometries: possibility of the method to deal with complex microstructures.
- Ease of discretization: most methods require a discretization of the RVE, which can be tricky in some cases.
- Accuracy of the macroscopic response: this is the main goal of the homogenization methods, so its accuracy is of first importance.
- Accuracy of the microfields: some methods, in addition to the prediction of the macroscopic response can give an accurate information about microfields as well.
- Computational cost: varies from a fraction of second to several hours on a multiprocessor computer so that it might be a huge limitation for applications of the method in practice.
- Nonlinear behaviors: the difficulty of extensions to nonlinear behavior greatly depend on the method.

An overview of the different methods is reported in table 2.1. Notice that by no way the list of the methods is exhaustive. Even if a lot of care has been taken to complete this table, some evaluations are still the subject of debate, especially when a method offers several variants. Furthermore, these evaluations are somehow subjective, a better solution would be to compare them on several benchmarks.

Homogenization method	2DFE	3DFE	2DVCFE	AHM
Complex geometries	+	+	+	+
Ease of discretization	++	+	+++	++
Accuracy macro response	++	+++	++	++
Accuracy microfields	+/++	+++	+	++
Computational cost	++	+	++	+
Nonlinear behaviors	+++	+++	+++	++
Homogenization method	GMC	HFGMC	FFTM	MFHM
Complex geometries	++	++	+++	++
Ease of discretization	++	++	+++	+++
Accuracy macro response	+++	+++	++	++
Accuracy microfields	+	++	++	+
Computational cost	++	+	+	+++
Nonlinear behaviors	+++	+++	++	++

Table 2.1: Comparison of different homogenization methods over various criteria. 2DFE: two-Dimensional Finite Element method, 3DFE: three-Dimensional Finite Element method, 2DVCFE: two-Dimensional Voronoi Cell Finite Element method, AHM: Asymptotic Homogenization Method, FFTM: Fast Fourrier Transform Method, GMC: Generalized Method of Cells, HFGC: High Fidelity Generalized Method of Cells and MFHM: Mean-Field Homogenization Method. Evaluations are: +: weak, ++: fair, +++: good.